Integration of Renewable Energy Resources to EV Using Sensor Less Control and Regenerative Braking

Indira Damarla(✉), Aare Anand, T. Thanmai Reethika, and H. Sai Niharika

Department of EEE, Velagapudi Ramakrishna Siddhartha Engineering College, Vijayawada, India
indira.damarla@gmail.com

Abstract. In this paper, a cutting-edge controller and drivetrain architecture for a renewable energy source (RES) powered Electric Vehicle (EV) has been proposed. Hall-Effect position sensor-less brushless dc (BLDC) motor drives frequently experience delayed commutation at low/high speeds. Conventional control is ineffective due to the small back EMF magnitude. The proposed technique uses the sensor with less control with commutation error compensation, driving the motor across the whole range. To identify the freewheeling pulses, a forward commutation error compensation algorithm has been created, which eliminates the requirement for low-pass filters and reduces the control complexity for low-cost EV applications. A separate phase compensator is not necessary because the use of the zero-crossing detection (ZCD) technology, which also automatically corrects the delay. The undesirable spikes in the ZCD circuit have been eliminated using a fixed delay digital filter. Effective MPPT control makes use of a modified landsman converter, which delivers ripple-free current at the output and eliminates the requirement for a ripple filter at the front end. The performance of the BLDC motor has been improved using the fuzzy logic-based PI controller. The efficiency of the suggested system is demonstrated using the MATLAB/Simulink environment.

Keywords: Dynamic response · Fuzzy PI controller · Brushless DC Motor · Landsman Converter · Regenerative braking · Sensor less control

1 Introduction

Electric vehicles are presently the most popular and an essential part of the nation's mass transit system. The battery capacity is a significant concern since it limits the vehicle's operational range [1–5]. The vehicle's energy is delivered to the battery and source. Increases in state of charge (SOC) can improve battery capacity rather than improving battery size, which would increase system weight and cost [6–9]. Brushless dc (BLDC) devices have often aroused significant interest in the EV space because to their high energy density and simple control design [10]. PI controller and switching signals that would provide pulse width modulation (PWM) are used to control the BLDC's speed

© The Author(s) 2023
B. Raj et al. (Eds.): ICETE 2023, AER 223, pp. 614–624, 2023.
https://doi.org/10.2991/978-94-6463-252-1_63

[11]. Commutation error is difficult to remove since the correctness of commutations is negatively impacted by several non-ideal factors [12]. This difficulty is addressed by sensor-less control is based on the third-harmonic compensation approach, which also improves the aesthetic attractiveness of the drive system [13]. At the source, power electronics converters manage power conversion. Semiconductor power elements in power converters are suitable for both low- and high-power applications [14]. Power converter problems include low efficiency, a large capacitor as well as other passive components. The landsman converter outperforms converters such as SEPIC, ZETA, and CUK since it uses fewer components and overcomes the aforementioned issues [15]. Pulse Width Modulation (PWM), Proportional Integral (PI), and Proportional Integral Derivative (PID) control can be used to control and regulate conventional systems. This further generates gate signals with the correct duty cycle for the power switches [16]. The system have being stabilized using fuzzy-PID controller in order for the landsman converter to increase the DC link voltage, shorten the falling period, and provide a steady input source for the Three Level Voltage Source Converter (VSC) [17]. The BLDC motor's sophisticated control and back EMF estimation are both incorporated into the basic Fuzzy-PID method implementation [18].

2 Proposed LC Fed BLDC Motor Drive System

As shown in Fig. 1, the recommended system uses a PV source to provide direct current to a brushless DC drive. The proposed drive system includes three level VSI, a landsman converter, a single diode PV array, wind with AC/DC, and a BLDC motor.

The LC controls high voltage gain before sending it to the VSI connected to the BLDC. The Fuzzy-PID control approach uses LC to provide high voltage. In this suggestion, high voltage gain and LC output voltage settling time are achieved using the fuzzy-PID control technique. The BLDC motor's speed and ripple control are controlled without the need of sensors.

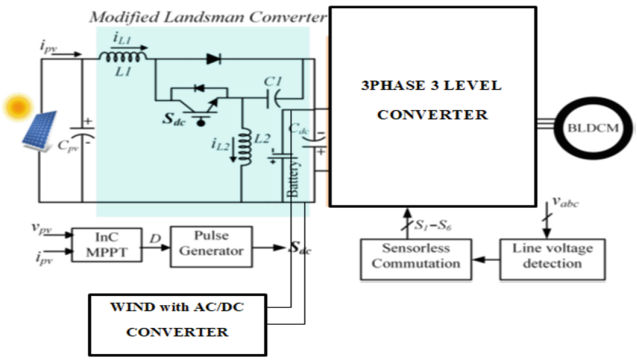

Fig. 1. Block diagram of proposed drive topology

3 Design of Landsman Converter

The LC is a dc-dc converter whose purpose is to increase photovoltaic (PV) power and whose performance in the CCM is dependent on the irradiance deviation level. The proposed LC gives brushless DC motors better voltage with reduced settling time. The suggested LC optimizes the PV array output voltage for a better, safer, and quieter BLDC motor operation. By virtue of the LC converter's function, the suggested BLDC system's DC bus voltage is regulated and increased voltage gain. LC converter consists of two Inductors (L_1, L_2), A switch (S_{dc}) and a capacitor C_1. The input of the LC converter is connected to the Solar output and output is Connected to the DC Capacitor (C_{dc}). The solar panel is rated for $V_{pv} = V_{mp} = 47$ V & $i_{pv} = I_{mp} = 8.11$A in terms of voltage and current, respectively. Because the revised Landsman converter's input inductor carries $i_{pv} = i_{L1} = 8.11$ A, the specified PV panel likewise carries that amount of current.

The following is assumed for the duty ratio of the dc-dc converter:

$$D = \frac{V_{dc}}{V_{dc} + V_{pu}} = \frac{48}{48 + 46.8} = 0.506 \tag{1}$$

where V_{dc} and v_{pu} are the voltages of a dc bus and also the PV panel output, respectively. The current flowing through the electrical connection capacitor while it is at full power is calculated as follows:

$$I_{dc} = \frac{P_{mp}}{V_{dc}} = \frac{380}{48} = 7.91A. \tag{2}$$

The frequency of 20 kHz is used to create PWM pulses for the converter. The terms I_{L1} and I_{L2} denote the inductor currents. Despite allowing a little amount of ripple to pass through the circuit to estimate component size, the output voltage ripple is limited by the large value of the dc bus capacitor. The VSI's maximum and minimum angular harmonics are employed to improve the DC bus capacitor. Table 1 demonstrates the process used for parameter designing the LC Converter.

Table 1. Specifications of Proposed Drive System

Parameter	Expression	Value
C_1	$\frac{D \times I_{dc}}{f_{sw} \times \Delta V_{dc}}$	42.09 μ F
L_1	$\frac{D \times I_{dc}}{8 \times f_{sw}^2 \times C_1 \times \Delta I_{L1}}$	73.98 μ F
L_2	$\frac{D \times V_{mp}}{f_{sw} \times \Delta I_{L2}}$	5.85 μH
C_{dc}	$C_h = \frac{I_{dc}}{6 \times \omega_h \times \Delta V_{dc}}$ $C_l = \frac{I_{dc}}{6 \times \omega_l \times \Delta V_{dc}}$	$C_h = 306.88\,\mu$ F $C_l = 1092.8\,\mu$ F $C_{dc} = 1000\,\mu$ F

3.1 PID Fuzzy Controller

In this paper, suggested PV converters for DC-DC and DC-AC contain a fuzzy-PID controller that is in control of a power switch (S). In EV applications, it may be used to address issues that make non-linearity and its interactive nature difficult to handle using traditional control approaches. This control exhibits all of the characteristics of this type of problem. Five attribute values (MF) for inputs and five MF for output fuzzy sets make up the five groups into which the fuzzy logic model parameters have been divided in Fig. 3. Using the Mamdani fuzzy inference approach, this system connects two input variables to one output variable. The error and the change of error (d), which denormalizes the data, are the two input variables (Fig. 2 and Table 2).

In contrast to simply understanding NB, NS, Z, PS, and PB to stand for negative big, negative small, zero, positive small, and positive large, respectively, this feature provides a hint as to how to use the interpolation of the basic table of rules to construct a more accurate continuous control rule.

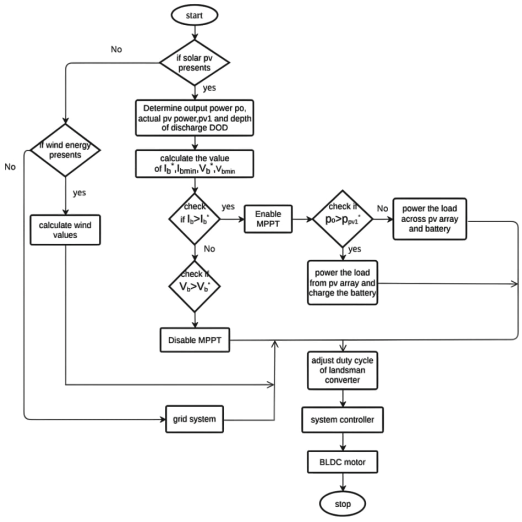

Fig. 2. Flow chart of the proposed system

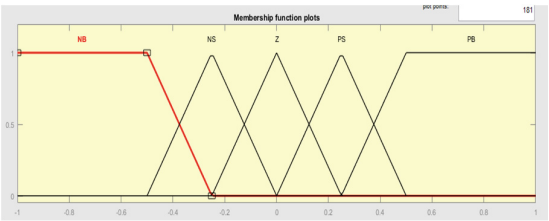

Fig. 3. Membership function of FLC

Table 2. Fuzzy Rule Base

Δwe	w_e				
	NB	NS	Z	PS	PB
NB	NB	NB	NS	NS	Z
NS	NB	NS	NS	Z	PS
Z	NS	NS	Z	PS	PS
PS	NS	Z	PS	PS	PB
PB	Z	PS	PS	PB	PB

4 Simulation Results & Discussion

The proposed LC converter with Fuzzy-PID has been simulated using Simulink model; BLDC motor driven by renewable PV array. Low PV module energy is fed to the landsman converter to regulate the high DC link voltage. For BLDC motors that run on the DC voltage generated by the converter supplied by the PV, VSI generates three phase voltages. Figure 4 represents the Simulink Implementation of Proposed Circuit the Parameters of the Proposed System is Illustrated in the Tables 3 and 4.

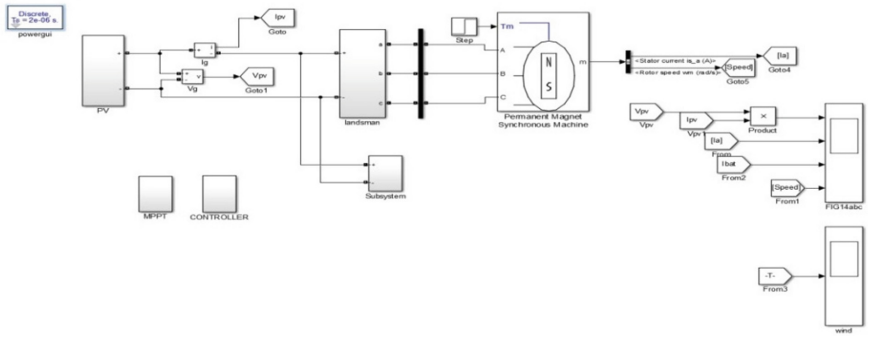

Fig. 4. Simulink Implementation of Proposed Drive System

Table 3. System Parameters

Parameter	Value
BLDC motor	48 V, 850 W, single speed, 7:1 gear arrangement
PV array	250 W
Battery pack	48 V, 100 Ah, Li-ion
Power converters	Modified Landsman converter rated at 2 kW and three-phase VSI capable at 10 kW

Table 4. BLDC Motor Specifications

Parameter	Value
Stator resistance	0.18 Ω
Stator inductance, (L)	50 mH
Motor constant	33.513
Torque /Amp rating	0.32
Pole pairs	2
Moment of Inertia (kg.m^2)	0.02

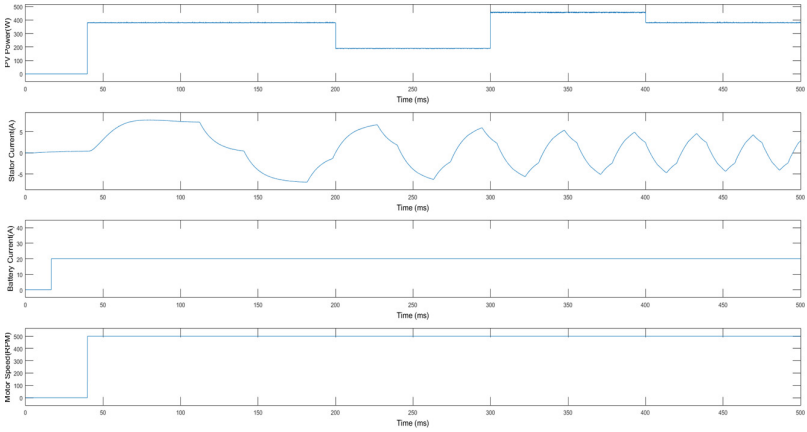

Fig. 5. Waveforms of PV Power, Stator Current, Battery Current, Motor Speed

4.1 Results of Solar PV System with MPPT Control

The input current to the drive is effectively regulated in line with the attainable solar irradiation. Power for the motor is simultaneously provided by a solar panel and a battery and wind which is Accomplished with AC-DC converter.

In Fig. 5 indicates that when declining solar irradiation, battery power increases in order to keep the motor speed constant. Similar to how power consumption from the battery decreases on a sunny day owing to available solar irradiation. Both transitory situations have the same speed. Throughout the procedure, 1.4 Nm of load torque is applied. A evaluation of converter electrical output with and without a fast load change. A redesigned Landsman converter with decreased ripple and quicker settling time provides improved stability. The output waveforms of the proposed system's three level inverter is shown Fig. 6.

4.2 BLDC Motor Drive Performance with Position Sensor Less

Figure 7 represents the proposed system's theta, stator, and speed under steady state conditions. The sensor less algorithm assumes control as soon as the rotor starts to

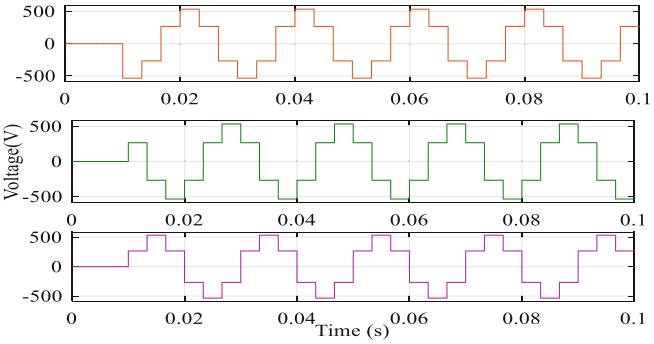

Fig. 6. Output waveform of three level inverter

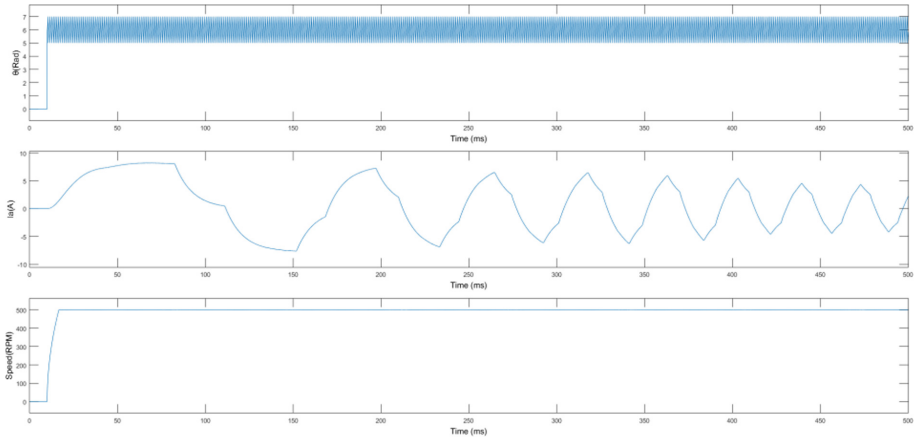

Fig. 7. Wave forms theta, Phase current, Speed

speed. By activating two phases using a predetermined commutation logic, the rotor is first aligned to a predetermined position.

Delivering the significant initial torque demanded by the EV requires a phase current that is nearly twice as high as the rated current. In comparison to the LPF-based drivel control, which needs 400 ms of induced acceleration time, our proposed method completes this work in roughly 230 ms. The initial value for the load condition is 3 Nm. The operating point, which limits any surge during startup, allows for a smooth and speedy start. The waveform of the proposed wind energy output subsystem is shown in Fig. 8.

4.3 Performance of Proposed Drive System at Different Speed Conditions

Figure 9 depicts the effect of the suggested commutation error-correcting logic on the phase current at various speeds. The suggested technique is compared to standard LPF-based delay compensating circuitry for this EV application, and a measurable decrease in current ripple is observed. At high speeds, the current ripple utilizing the technique

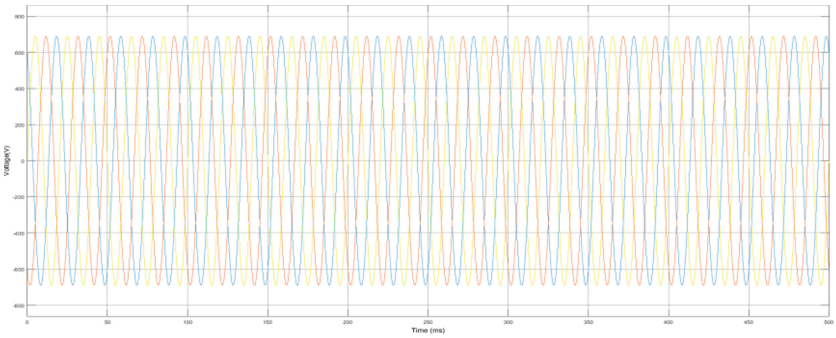

Fig. 8. Output waveform of wind energy

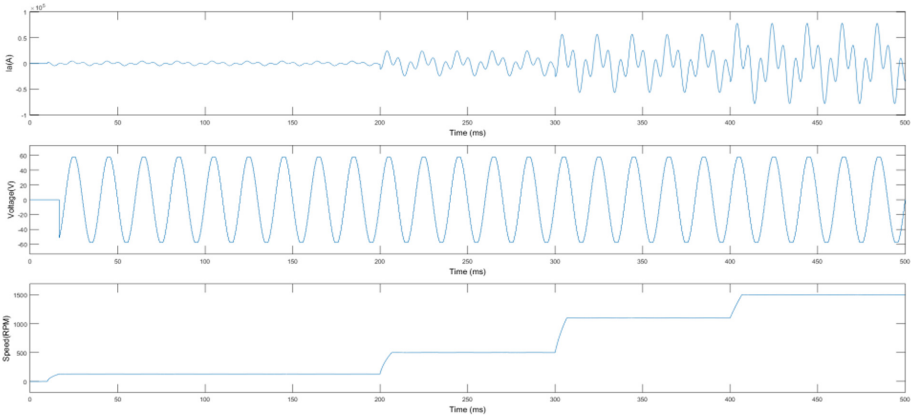

Fig. 9. Performance of proposed drive system under different speed conditions at 130 rpm, 500 rpm, 1100 rpm

gets worse. This is caused by the flawed ZCPs. The imbalanced dc link voltage and the technology's calculation delay are to blame for the current spike that occurs during synchronization, even though the LPF-based technique also compensates for the delay. The suggested approach preserves the present profile's form and keeps the current ripple under control. As a result, the suggested compensation approach eliminates current spikes and makes the sensor less commutation of the BLDC motor drive better.

4.4 Performance of Proposed Drive System at Different Load Conditions

Figure 10 illustrates the drive's dynamic performance as the load varies. It is seen when the load rises to the rated 2.6 Nm since there is an increase in current and a slight decrease in speed. Current decreases as the load is lowered to half of the rated torque. Dc bus voltages are stable in both scenarios, indicating that speed is stable in stable equilibrium. But during transient, there is a tiny overshoots and under shoot of speed for a brief period of time.

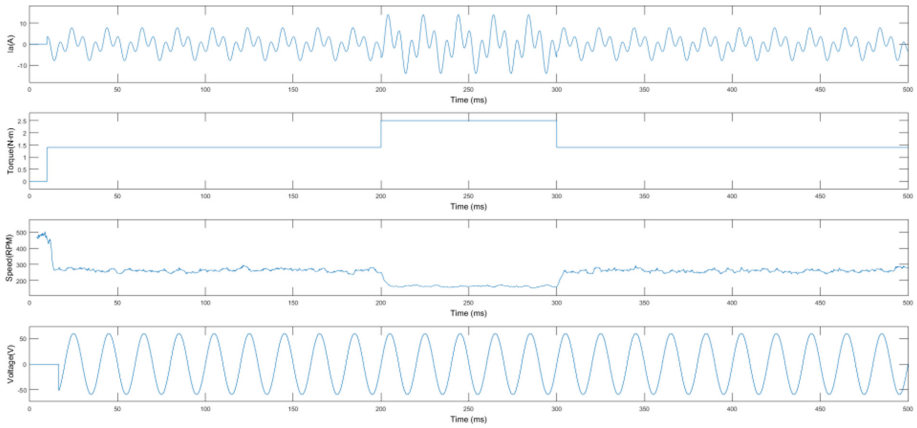

Fig. 10. Phase current I_a, Torque, Speed, Phase Voltage V_{ab}

5 Conclusion

The steady-state and dynamic characteristics of the proposed solar PV array-based BLDC motor-driven EV with a Landsman converter have been examined in this work. By using a Landsman converter, it is no longer necessary to use external filters, and it also helps to reduce oscillations in the module current that result from snubber components. The hybrid PV-wind system being study is built to entirely self the load during operation. The performance of the proposed system was demonstrated by the simulation results produced by MATLAB SIMULINK. The outcomes demonstrated that the solar and wind generators could provide the load with the necessary energy and charge the battery. Using the voltage level and the dc bus voltage, this position Sensor less control calculates commuting points. Any imbalance or change in the bus voltage causes erroneous commutation, significant pulse duration, and a variable frequency curve. The suggested method significantly eliminates current disturbances, results in a reliable and smooth sensor less commutation. This technique minimizes interference pulses by estimating the commutation time using freewheeling signals. The MPPT performance of the upgraded Landsman converter has significantly improved. Furthermore, the system is extremely energy-efficient because of the regenerative braking. Therefore, the suggested approach is practical and suitable for BLDC vehicle applications for low-Price light electric cars.

References

1. S. Chen, X. Zhou, G. Bai, K. Wang, and L. Zhu, "Adaptive commutation error compensation strategy based on a flux linkage function for Sensorless brushless DC motor drives in a wide speed range," IEEE Trans. Power Electron., vol. 33, no. 5, pp. 3752–3764, May 2018.
2. M. H. Bierhoff, "A general PLL-type algorithm for speed Sensorless control of electrical drives," IEEE Trans. Ind. Electron., vol. 64, no. 12, pp. 9253–9260, Dec. 2017.
3. X. Zhou, X. Chen, C. Peng, and Y. Zhou, "High performance non salient sensorless BLDC motor control strategy from standstill to high speed," IEEE Trans. Ind. Inform., vol. 14, no. 10, pp. 4365–4375, Oct. 2018.

4. P. Li, W. Sun, and J.-X. Shen, "Flux observer model for sensorless control of PM BLDC motor with a damper cage," IEEE Trans. Ind. Appl., vol. 55, no. 2, pp. 1272–1279, Mar. 2019.
5. S. Ogasawara and H. Akagi, "An approach to position sensorless drive for brushless DCmotors," IEEE Trans. Ind. Appl., vol. 27, no. 5, pp. 928–933, Oct. 1991.
6. Indira D and Venmathi M, "A Comprehensive Survey on Hybrid Electric Vehicle Technology with Multiport Converters", Emerging Trends in Computing and Expert Technology, Lecture Notes on Data Engineering and Communications Technologies, Springer, vol. 35, pp. 70–85, Nov 2019.
7. B. Saha and B. Singh, "Solar PV integration to e-rickshaw with regenerative braking and sensorless control," in Proc. IEEE 17th India Council Int. Conf., Dec. 2020, pp. 1–6.
8. L. Yang, Z. Q. Zhu, H. Bin, Z. Zhang, and L. Gong, "Virtual third harmonic back EMF-based sensorless drive for high-speed BLDC motors considering machine parameter asymmetries," IEEE Trans. Ind. Appl., vol. 57, no. 1, pp. 306–315, Jan. 2021.
9. X. Zhou, X. Chen, F. Zeng, and J. Tang, "Fast commutation instant shift correction method for sensorless coreless BLDC motor based on terminal voltage information," IEEE Trans. Power Electron., vol. 32, no. 12, pp. 9460–9472, Dec. 2017.
10. Modeling and Control PV-Wind Hybrid System Based On Fuzzy Logic Control Technique Doaa M. Atia, Faten H. Fahmy, Ninet M. Ahmed, Hassen T. Dorrah. Vol.10, No.3, September 2012, pp. 431~441.
11. Photovoltaic Based Landsman Converter With Fuzzy Logic Controller Fed Bldc Motor For Water Pumping Applications
12. Fuzzy logic power management for a PV/wind microgrid with backup and storage system-sISSN: 2088–8708, DOI: https://doi.org/10.11591/ijece.v11i4.pp2876-2888
13. Solar photovoltaic array fed water pump driven by brushless DC motor using Landsman converterIET Renew. Power Gener., 2016, Vol. 10, Iss. 4, pp. 474–484
14. Design of Fuzzy-Pid with Landsman Converter (LC) Fed BLDC Drive Using IFOC Controller IOP Conf. Series: Materials Science and Engineering 925 (2020) 012021 IOP Publishing. Doi: https://doi.org/10.1088/1757-899X/925/1/012021.
15. Design and Analysis of High Gain Interleaved DC-DC Converter for Solar Powered Sensorless BLDC Pump.
16. An Intensified Marine Predator Algorithm (MPA) for Designing a Solar-Powered BLDC Motor Used in EV Systems. https://doi.org/10.3390/su142114120.
17. P. P. Acarnley and J. F. Watson, "Review of position-sensorless operation of brushless permanent-magnet machines," IEEE Trans. Ind. Electron., vol. 53, no. 2, pp. 352–362, Apr. 2006.
18. S.Chen, G. Liu, and L. Zhu, "Sensorless control strategy of a 315kW highspeed BLDC motor based on a speed-independent flux linkage function," IEEE Trans. Ind. Electron., vol. 64, no. 11, pp. 8607–8617, Nov. 2017.

Open Access This chapter is licensed under the terms of the Creative Commons Attribution-NonCommercial 4.0 International License (http://creativecommons.org/licenses/by-nc/4.0/), which permits any noncommercial use, sharing, adaptation, distribution and reproduction in any medium or format, as long as you give appropriate credit to the original author(s) and the source, provide a link to the Creative Commons license and indicate if changes were made.

The images or other third party material in this chapter are included in the chapter's Creative Commons license, unless indicated otherwise in a credit line to the material. If material is not included in the chapter's Creative Commons license and your intended use is not permitted by statutory regulation or exceeds the permitted use, you will need to obtain permission directly from the copyright holder.